Nd^{3+} crystal-field transitions studied by Raman and FIR spectroscopies in Nd_2BaZnO_5

A. de Andrés, S. Taboada, and J. L. Martínez
Instituto de Ciencia de Materiales de Madrid, Consejo Superior de Investigaciones Científicas, Campus de Cantoblanco, Madrid, E-28049 Spain

M. Dietrich, A. Litvinchuk, and C. Thomsen
Institut für Festkörperphysik, TU-Berlin, Hardenbergstrasse 36, 10623 Berlin, Germany
(Received 10 May 1996)

We have investigated the crystal-field levels of the lowest multiplets of Nd^{3+} in the Nd_2BaZnO_5 compound. Raman scattering arising from the excitation of the ground-state level to several $I_{9/2}$, $I_{11/2}$, and $I_{13/2}$ levels has been observed as a function of the temperature. Fourier-transform infrared reflectivity (between 30 and 7000 cm^{-1}) has been measured down to 30 K. Bands corresponding to transitions from $I_{9/2}$ to $I_{11/2}$, $I_{13/2}$, and $I_{15/2}$ multiplets were obtained and are in very good agreement with the observed Raman crystal-field transitions (CFT). The first excited state at 65 cm^{-1} becomes detectable in Raman scattering as the temperature decreases, i.e., as its thermal population decreases. It is also observed that the intensity of IR absorption peaks from this level decreases with temperature, as expected, but some are still detectable, even at 30 K. The width of the 65 cm^{-1} Raman peak is larger than all other observed Raman CFT in this compound. This width is due to its proximity to the ground state, i.e., to the high probability of relaxation. A small component of inhomogeneous broadening due to slight differences in Nd environments is also present. The possible coupling between this CFT and a near phonon is discussed. [S0163-1829(97)04406-8]

INTRODUCTION

Oxides with the R_2BaMO_5 formula, where R is a rare earth and M a transition metal, crystallize in only a few space groups. The major part of cuprates show the most complicated structure, which is orthorhombic ($Pnma$, $Z=4$).[1] Cuprates with La and Nd, which are the lanthanide ions with larger ionic radii, present a tetragonal $P4/mbm$ (Ref. 2) structure, with a coordination of four oxygen ions forming planar squares. Recently, La and Nd zinc oxides have been prepared and are found to belong also to a tetragonal space group ($I4/mcm$) with ZnO_4 tetrahedra and two formulas per primitive cell.[3] The optical phonons of most of these R_2BaMO_5 compounds have been studied in Refs. 4 and 5.

The crystal-field levels of the $4f$ electrons of rare earth ions introduced as dopants in solid matrix are extensively studied. These electronic levels have the property of being very localized, but also influenced by the electric and magnetic order around the rare earth ion, so that their study can give information on the local order (different environments due, for example, to their position at different crystal sites or to defects in the first coordination sphere), and also on long-range interactions such as magnetic order in the crystal. Now, their study in high-T_c superconductors, where the rare earth is a component of the crystal, is of increasing interest.

A study of the relation between the electronic transitions in Eu_2BaCoO_5, Eu crystal field, and interband transitions and the optical phonons was reported in Ref. 6. An extensive investigation of the interaction between Raman phonons and crystal-field transitions has been done for the $NdBa_2Cu_3O_{7-d}$ compound.[7] The Raman crystal-field transitions have also been used to study the different environments of Pr ions in $Pr_{1.85}Ce_{0.15}CuO_4$ compound.[8] A further publication[9] explains the observed splitting of Nd Kramers doublets due to Nd-Cu exchange interaction in Nd_2CuO_4. Visible absorption experiment in Nd_2BaZnO_5 has been reported in Ref. 10.

The ground-state and lower multiplet crystal-field split levels are often obtained as energy differences between absorption or emission peaks observed in the visible or near-IR range. On the contrary, Raman crystal-field transitions (CFT) are direct evidence for transitions between the lowest levels, such as absorption processes from the ground-state to the low-energy excited levels.

The aim of this work was twofold: one was to test, in a compound which has a composition similar to high-T_c superconductors, the possibilities of the Raman and IR techniques applied to detect the CF levels. Luminescence spectra obtained with standard techniques are often, in this kind of compound, not detectable. The second point was to analyze the relation between Raman and IR peaks and to observe and explain the behavior of the intensity of the Raman transitions with the temperature as well as the interaction between the different elementary excitations in a complex, but still manageable and well-defined system.

EXPERIMENTAL DETAILS

The Nd_2BaZnO_5 oxide was prepared as a polycrystalline sample, mixing the stoichiometric amounts of the high-purity oxides, Nd_2O_3 (99.999%), ZnO (99.99%), and $BaCO_3$ (99.999%). The homogenized mixture was heated in air at 950 °C for 12 h, then it was reground and reheated at 1050 °C for another 12 h. Once the powder was pressed into a pellet, a third thermal treatment at 1000 °C was achieved in order to obtain a compacted ceramic. The x-ray diffraction data show that the sample is single phase (up to the usual limits of this technique) and presents the $I4/mcm$ structure. The as grown polycrystalline sample is white, which is an indication that it is a wide-gap insulator.

The Raman-scattering experiments were performed with

an X-Y Dilor multichannel spectrometer with a photodiode array using a coherent Ar^+ laser as excitation source. The spectra were recorded at temperatures between 300 and 10 K in backscattering geometry using a continuous-flow Oxford Instrument cryostat. All spectra have been corrected by the spectral response of the experimental setup.

Reflectivity measurements were carried out on a Bruker-66v Fourier-transform interferometer in the range 30–7000 cm^{-1}. DTGS and MCT detectors were used. The sample was mounted on the cold finger of a temperature-variable cryostat.

RESULTS AND DISCUSSION

In this compound (with space group D_{4h}^{18}), the first coordination sphere of Zn is formed by four oxygen ions in irregular tetrahedra. The Nd ions are located at C_{2v} sites with eight oxygen ions as first neighbors and two Nd-O different distances [Fig. 1(a)]. In this low symmetry environment, the degeneracy of the Nd multiplets of the $4f$ configuration is completely split by the crystal field acting on the ions, except for the spin degeneracy that can be lifted only by an internal or external magnetic field acting at the Nd site. Therefore, we expect $(2J+1)/2$ Kramer's doublets for each free ion multiplet. This compound does not present any structural-phase transition. The magnetic behavior [Fig. 1(b)] is that of a paramagnet with weak antiferromagnetic correlations ($T_\theta = -40$ K) between the Nd ions where the crystal-field effects appear below 50 K. No ferromagnetic impurity phase is found down to 1.8 K.

The point group of the crystal is D_{4h} and has the inversion symmetry operation. The Raman modes are classified in the A_{1g}, B_{1g}, B_{2g}, and E_g irreducible representations. A transition between two electronic levels is Raman allowed if the direct product of their representations contains some of the irreducible representations of the Raman-active phonons. In the notation of double groups (for example, Ref. 11), the symmetry of all split $I_{J/2}$ levels for a C_{2v} site is Γ^5. The direct product of two of these levels is $\Gamma^5 \otimes \Gamma^5 = A_1 + A_2 + B_1 + B_2$, which correspond to $A_{1g} + B_{2g} + E_g$ for the D_{4h} point group. Therefore, all possible transitions, intra- and intermultiplets, are Raman allowed, and the transitions can couple to lattice phonons. On the other hand, the electric dipole has the $\Gamma^1(A_1)$, $\Gamma^2(A_2)$, and $\Gamma^4(B_2)$ representations, so infrared transitions between two Γ^5 levels are also allowed.

In Fig. 2 we present the evolution with the temperature of the 40–200 cm^{-1} region of the Nd_2BaZnO_5 Raman spectrum. The excitation was achieved with the 514.5 nm Ar^+ laser line. The same kind of spectra are obtained with the 488 and 457.9 nm excitation lines. The formation of a new peak at 65 cm^{-1} is observed as the temperature decreases, below the 80 cm^{-1} phonon. The Raman modes at room temperature of this compound have been observed and assigned in microcrystals;[5] according to these authors, no phonon is observed nor expected at 65 cm^{-1}. The spectra have been normalized by the incident power and the dotted curves (in Fig. 2) are also corrected by the Bose-Einstein occupation number for Stokes processes $[n(wT)+1]$ showing that the changes in intensity of the peaks above 70 cm^{-1} obey the temperature factor for first-order phonons. On the contrary,

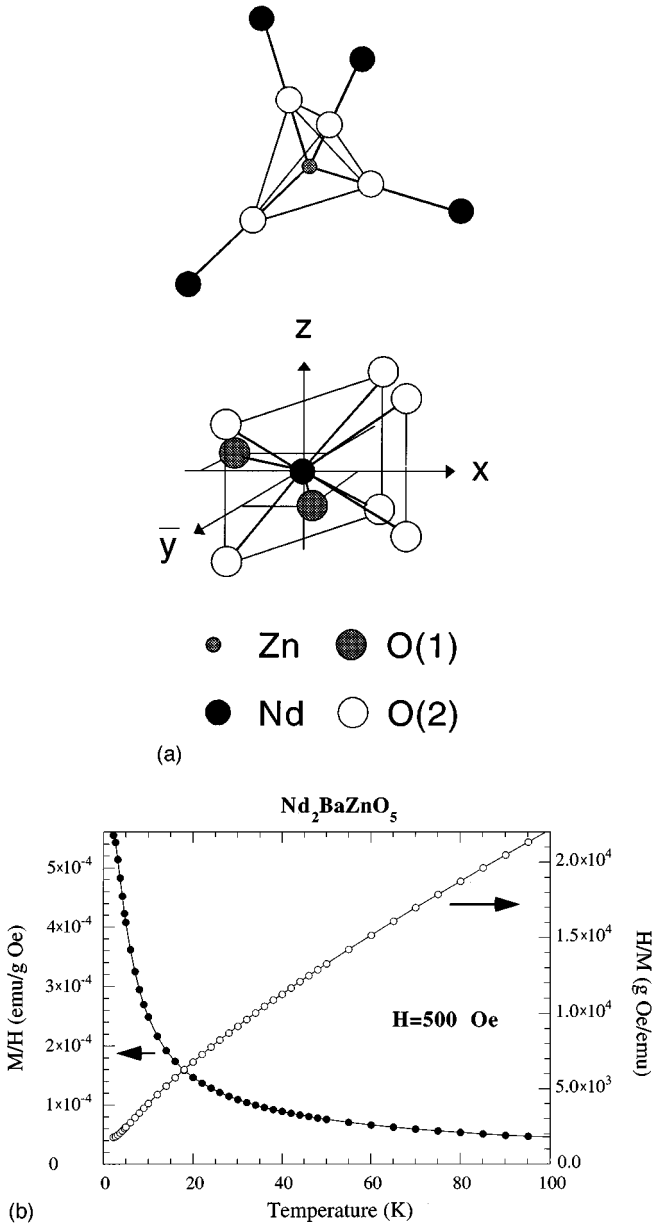

FIG. 1. (a). Environments of Zn and Nd ions in tetragonal Nd_2BaZnO_5. (b) Magnetic susceptibility and its inverse down to 1.8 K.

the intensity of the peak at 65 cm^{-1} increases on decreasing the temperature. We assign this peak to the Raman transition from the Nd^{3+} ground state to the first excited level (both levels belong to the $^4I_{9/2}$ free ion multiplet).

The electronic population of the 65 cm^{-1} level at room temperature n (300 K, 65 cm^{-1}) is quite large, and its lifetime is, because of its low energy, very probably short. As the temperature decreases, its population decreases and its lifetime increases, so that the detection of a peak corresponding to a transition between the ground state and this first excited state is more and more favorable, as is observed experimentally.

Figure 3 represents the expected (lines) and experimentally measured (symbols) temperature dependence of 500, 102, and 80 cm^{-1} phonons and 65 cm^{-1} CFT intensities. The peaks have been fitted to Lorentzian lines and their areas

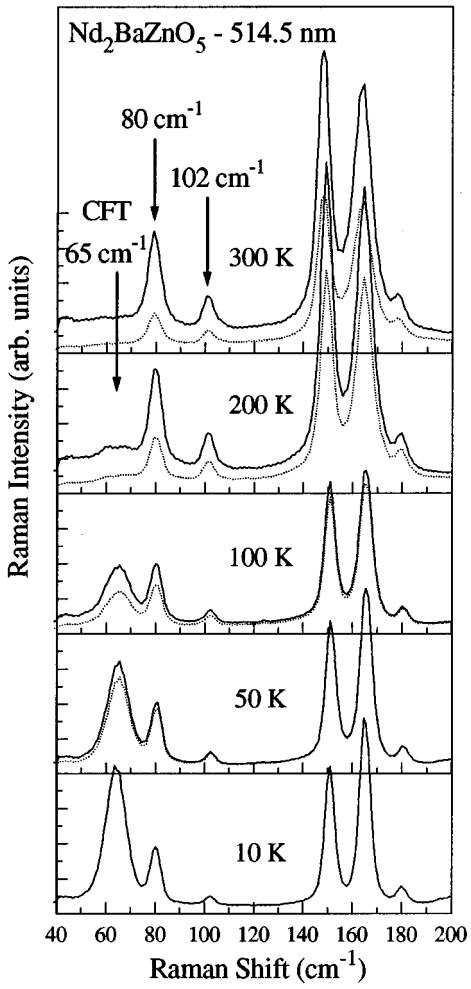

FIG. 2. Raman spectra of the Nd_2BaZnO_5 sample at different temperatures (solid lines) under 514.5 nm excitation. Dotted curves are the Raman spectra corrected by the Bose-Einstein thermal factor. A Nd CFT (crystal-field transition) is observed at 65 cm^{-1}, and two lattice phonons are indicated with arrows.

normalized to the 10 K values. Raman intensity due to one phonon process is proportional to the thermal occupation factor $1/(1-\exp[-h\nu/k_B(T)]$. The three upper lines represent this factor for three different phonons at 80, 102, and 500 cm^{-1}. On the other hand, the Raman intensity due to a crystal-field transition depends on the population of the involved levels. As in a usual absorption process, the probability of transition from a level l to a level k (W_{lk}) is proportional to the occupation of level l (N_1). In equilibrium, the population of the levels obey Boltzmann statistics: $N_1 = \exp(-E_1/k_BT)/[\Sigma_j \exp(-E_j/k_BT)]$, where the summation is over all atomic levels. Considering in this case only two levels, the ground state E_1 at 0 cm^{-1} and the first excited state E_k at 65 cm^{-1}, the population of the ground state is reduced to $N_1 = 1/[1+\exp(-65\ cm^{-1}/k_BT)]$, which is represented as the lower continuous line in Fig. 3. The other levels of the Nd^{3+} ground-state multiplet are usually at energies higher than 200 cm^{-1}, so their effect in N_1 is very small at temperatures below 200 K. The dotted curve is the population of the ground state considering a third level at 200 cm^{-1}. It can be observed that the agreement between the experimental normalized intensities and the calculated dependence

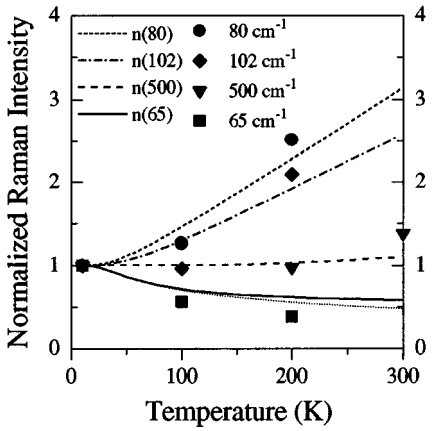

FIG. 3. Expected (lines) and experimentally measured (symbols) temperature dependence of 500, 102, and 80 cm^{-1} phonons and 65 cm^{-1} CFT intensities. The areas of the peaks are normalized to their 10 K values. The three upper lines represent the thermal occupation factor for first-order phonons and the lower line is the probability for an absorption process, taking into account the thermal occupation of a two-level scheme (0) and 65 cm^{-1}).

of the intensities with the temperature is quite correct.

In the present case, the energies of both excitations are temperature independent and the variation of their intensities can be relatively well explained by temperature population (Fig. 3). Nevertheless, if one compares the Raman spectra of Nd and La compounds (Fig. 4), a large shift (10 cm^{-1}) in the lowest phonon, at 80 cm^{-1} in Nd and 70 cm^{-1} in La compound, can be observed while the other low-energy phonons (below 300 cm^{-1}) change less than 3 cm^{-1}. The lowest phonon, of E_g symmetry, is tentatively assigned[5] to Ba vibration because this ion has the lowest charge-mass ratio. The environment of Ba ion is a ten-oxygen polyhedron with two Ba-O distances. The only movement allowed for the Ba ion is in the xy plane, so only one kind of Ba-oxygen (called O_2)

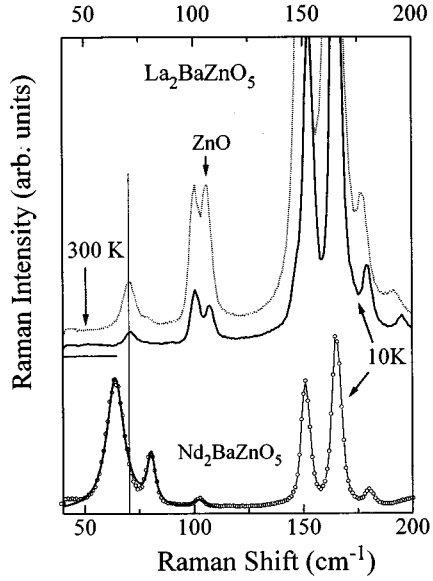

FIG. 4. Raman spectra of La_2BaZnO_5 compound at 300 and 10 K (upper curves) and of Nd_2BaZnO_5 at 10 K (lower curve) under excitation at 514.5 nm.

bond is involved in the Raman mode, which must be of E_g symmetry. A rough estimation of the effect of the change in the frequency due to the different bond lengths in both compounds (2.931 and 2.981 Å, respectively, for Nd and La), can be done considering a d^{-3} dependence of the force constant, where d is the bond length. This estimation would explain a change of only 1.5 cm^{-1} in the Ba vibration. A possible explanation of this considerable frequency shift is the coupling between this phonon and the Raman CFT observed at 65 cm^{-1}. The energies of both excitations are renormalized due to their interaction, in this case, increasing the phonon energy from the expected 71.5 cm^{-1} to 80 cm^{-1}. The deviation of the temperature behavior of the intensities of both peaks from the expected one (the intensity of the CFT increases more than expected upon decreasing the temperature, and that of the phonon decreases more) could be due to a transfer of intensity from one process to the other.

The width of the 65 cm^{-1} peak (FWHM=15 cm^{-1}) is larger than that of other observed CFT around 2000 cm^{-1} (FWHM=10 cm^{-1}), and also larger than the phonon's width (FWHM=5 cm^{-1}) at the lowest measured temperature. The width of this transition increases with the temperature. This can be understood taking into account the increase of the nonradiative transition probability from the 65 cm^{-1} level to the ground state with the temperature, which is related to the lifetime of this level. In fact, in the present case, it is very probably the most important contribution to the observed width. For transitions between $4f$ levels, the temperature dependence of the nonradiative rate is given by $N(T)=N(0)(1+n)^p$, where $p=(E_k-E_l)/h\nu$, and $(1+n)$ is the phonon occupation factor.[12] In the present case, the exponent p is near 1, since the small energy difference between the two levels assures the existence of phonons (optic or acoustic) of the correct energy. Therefore, in a first approximation $N(T)$ is proportional to $(1+n)$, which is the same factor as the one calculated in Fig. 3 for the temperature dependence of phonons. We have not analyzed in detail the evolution of the widths because the data are not of sufficient quality to obtain more information. Nevertheless, the qualitative behavior of the width of the 65 cm^{-1} peak indicates that the lifetime of the excited level is understood, considering its high nonradiative probability of relaxation, even at 10 K, and its increase with the temperature related to the increase of the population of phonons of similar energy.

Nevertheless this peak does not fit exactly to a Lorentzian curve; a small Gaussian component is necessary: Figure 4 presents the fit to three Lorentzian curves of the three first peaks of the Nd sample; the wings of the 65 cm^{-1} peak are not well fitted. This is an indication that besides the width related to the lifetime of the level, an inhomogeneous broadening, due to slightly different environments of Nd ions in Nd_2BaZnO_5, is present.

Figure 5 presents the IR reflectivity in the 0–6000 cm^{-1} region at room temperature. The upper part shows the phonon region, demonstrating the good quality of the obtained spectrum. Above the phonon region, the reflectivity should be a constant related to the ε_{inf} value. The departure from that value is due to two effects: one is the fact that the sample is a pellet, so as the wavelength is shorter, it becomes first comparable and later smaller than the grain size and the reflectivity decreases; there is no longer one interface, but a

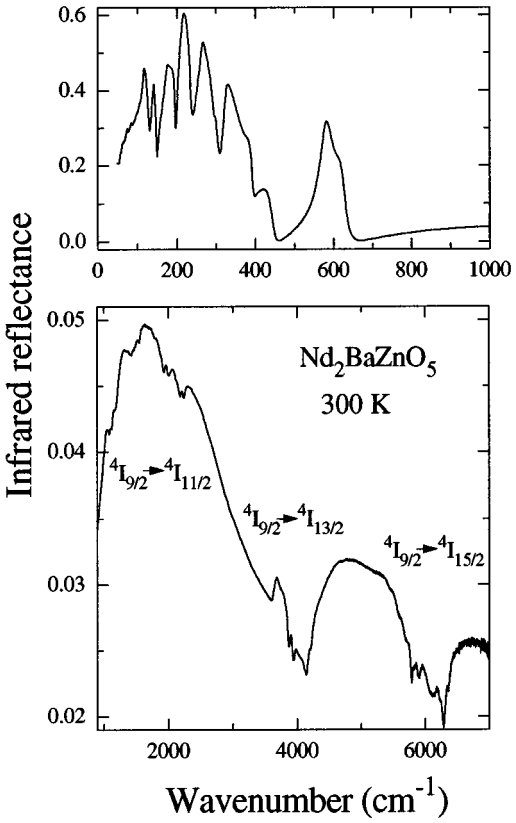

FIG. 5. Infrared reflectivity at 300 K of Nd_2BaZnO_5 compound. The upper part shows the phonon range and the lower part Nd^{3+} crystal-field absorption depths from the $I_{9/2}$ ground state multiplet to the $I_{11/2}$, $I_{13/2}$, and $I_{15/2}$ multiplets.

set of individual microcrystals. The other is caused by the absorption of Nd ions in the crystal. These absorption dips correspond to transitions from the ground-state multiplet $I_{9/2}$ to the first three excited multiplets $I_{11/2}$, $I_{13/2}$, and $I_{15/2}$.

In Fig. 6 we compare the Raman and IR spectra in the region of the first excited multiplet. The lower part of Fig. 6 shows the Raman spectra at 10 K, for two excitation energies, 457.9 and 514.5 nm. Raman CFT are observed at constant Raman shift for different excitation energies, as phonons, while luminescence peaks appear at constant absolute energy (laser-Raman shift). It is clear that the peaks around 2000 cm^{-1} are Raman CFT. The three upper curves in Fig. 6 are infrared reflectivity spectra at different temperatures (300, 100, and 30 K), in the $I_{9/2}$ to $I_{11/2}$ transition energy range. We have labeled 1 to 6 the peaks corresponding to the ground state to the six levels of the $I_{11/2}$ multiplet. The peaks connected by a curved arrow are transitions to the same final state (levels 1, 2, and 3 of $I_{11/1}$), but coming from a different initial state: the peaks observed at higher energy come from the ground state, and those at lower energy from the 65 cm^{-1} first excited state. Comparing the 100 and 30 K spectra, it is clear that the intensity of these last peaks decreases with the temperature, which is the expected behavior, since the electronic population of the 65 cm^{-1} also decreases. Nevertheless, the decrease is smaller than expected, considering only the thermal population of the 65 cm^{-1} level (equal to 1 plus the population of the ground state of Fig. 3). It is again necessary to take into account the effect on the nonradiative relaxation from the 65 cm^{-1} level. The tem-

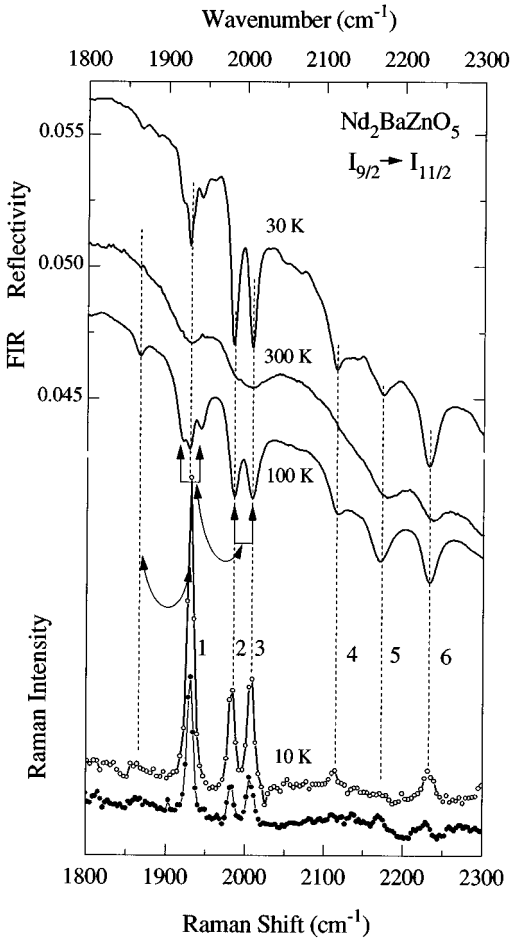

FIG. 6. Infrared reflectivity at 300, 100, and 30 K (three upper lines) and Raman scattering for two excitation energies (457.9 and 514.5 nm) at 10 K (dotted curves) in the $I_{9/2}$ to $I_{11/2}$ transitions region. The peaks numbered from 1 to 6 correspond to transitions between the 0 cm^{-1} ground level to the six $I_{11/2}$ levels. The curved arrows relate the transitions to the same excited level but coming from the 0 and 65 cm^{-1} levels. The three IR curves are plotted in the same scale, but a vertical shift is included to facilitate the vision.

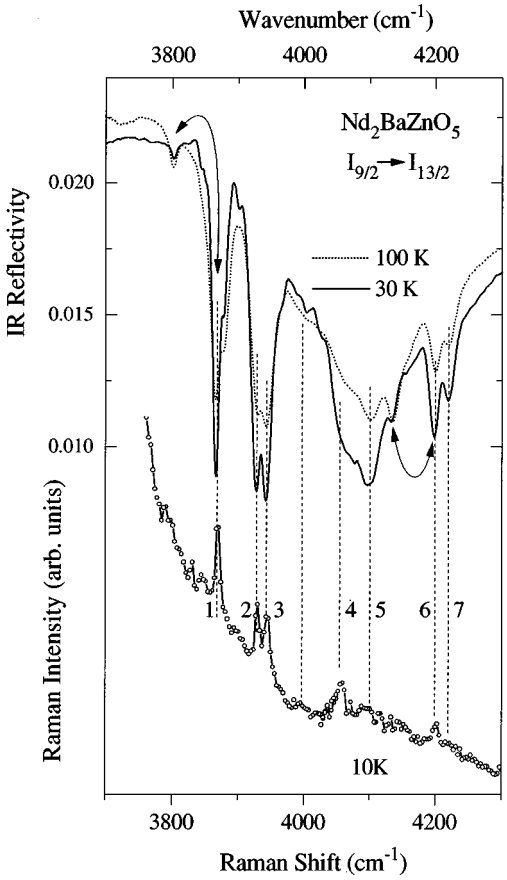

FIG. 7. Infrared reflectivity at 100 and 30 K (upper lines) and Raman scattering at 10 K (dotted curve) in the $I_{9/2}$ to $I_{13/2}$ transitions region. The peaks numbered from 1 to 7 correspond to transitions between the 0 cm^{-1} ground level to the seven $I_{13/2}$ levels. The curved arrows relate the transitions to the same excited level, but coming from the 0 and 65 cm^{-1} levels.

perature increases the nonradiative relaxation (a factor 3 between 30 and 300 K in this case) so that, on one hand, the lifetime of the atomic level decreases and the related peaks broaden, and on the other hand, the intensity of a radiative transition (emission or absorption) from this level decreases.

In Fig. 7 we present the IR reflectivity spectra at 100 K and 30 K (upper curves) and Raman spectrum at 10 K for 457.9 nm excitation wavelength (lower curve) in the $I_{9/2}$ to $I_{13/2}$ transition energy region. We can index the seven levels of the $I_{13/2}$ multiplet (1–7 in Fig. 7). Again, some transitions from the 65 cm^{-1} level are observable; two of them are indicated with curved arrows. The $I_{9/2}$ to $I_{15/2}$ transitions are observed in the IR reflectivity spectra of Fig. 8. The Raman spectra do not show these Raman CFT; they may be hidden by luminescence peaks. All observed Raman CFT are quite weak, so that only the most efficient transitions are detectable, even if all are allowed.

Table I summarizes the obtained CF levels of the Nd^{3+} ion in Nd_2BaZnO_5 compound detected by Raman scattering and/or by infrared reflectivity. A transition observed with both techniques at 988 cm^{-1} (not shown in the figures) is

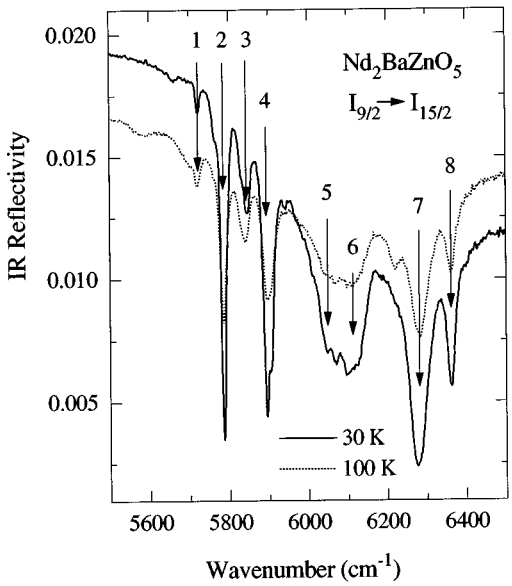

FIG. 8. Infrared reflectivity at 100 and 30 K in the $I_{9/2}$ to $I_{15/2}$ transitions region. The peaks numbered from 1 to 8 correspond to transitions between the 0 cm^{-1} ground level to the eight $I_{15/2}$ levels.

TABLE I. Observed Nd crystal-field levels obtained from Raman scattering (R) and/or infrared reflectivity (IR). (b)=broad.

Multiplet	Level no.	Level energy (cm^{-1})	Raman/IR
$^4I_{9/2}$	1	0	
	2	65	R
	5	(988)	IR/R
	1	1929	IR/R
	2	1983	IR/R
$^4I_{11/2}$	3	2008	IR/R
	4	2115	IR/R
	5	2174	IR
	6	2232	IR/R
	1	3868	IR/R
	2	3928	IR/R
	3	3941	IR/R
$^4I_{13/2}$	4	4055	IR(b)/R
	5	4100	IR(b)
	6	4200	IR/R
	7	4220	IR
	1	5722	IR
	2	5784	IR
	3	5842	IR
$^4I_{15/2}$	4	5896	IR
	5	6050	IR(b)
	6	6109	IR(b)
	7	6283	IR
	8	6362	IR

included in the table (in parentheses) as a fifth level corresponding to the $I_{9/2}$ multiplet. Nevertheless, this value is very high, i.e., the splitting of the lower multiplet is unusually large if we compare it with data on Nd in other compounds.

The general level scheme obtained by both techniques for the $I_{J/2}$ multiplets of Nd is similar to those in other compounds. The CFT do not show a splitting due to the weak antiferromagnetic interactions present in the sample; they are probably too weak to produce a detectable splitting with our experimental systems.

CONCLUSIONS

The presented studies demonstrate the utility of Raman and IR spectroscopies for the direct determination of the lowest crystal-field levels of rare earth ions, in the cases where luminescence and standard absorption techniques are not suitable for their direct observation because of the very low energy of the involved transitions. IR spectroscopy has been used to determine the lowest multiplets of rare earth ions, which are constituents of the compound. The combination of both techniques has allowed us to obtain the CF levels of the ^4I_J ($J=\frac{9}{2}$ to $\frac{15}{2}$) multiplets in tetragonal Nd_2BaZnO_5 where all possible transitions between these crystal-field levels, which are Kramers doublets of Γ^5 symmetry, are Raman and IR allowed.

It has been obtained that the intensity of the Raman crystal-field excitation associated with the transition from the ground state to the first excited state, 65 cm^{-1} above, follows quite well the variation of the population factor of the ground state, in a two-level scheme, with the temperature, but not exactly. The departure from this behavior, together with the frequency of the lowest phonon (80 cm^{-1}), higher than expected in comparison with the La compound, could be due to a coupling between both elementary excitations. The width of the Raman crystal-field peak at 65 cm^{-1} is related to the short lifetime of the excited level due to the high probability for the nonradiative relaxation process from this level. A small component of inhomogeneous broadening due to slight differences in Nd environments is also present. This variation of the lifetime of the excited level with the temperature also explains the dependence of the intensity of the absorption dips in the IR spectra which correspond to transitions from the 65 cm^{-1} level.

ACKNOWLEDGMENTS

We acknowledge financial support from the C.I.C.y.T. (Ministerio de Educación y Ciencia) under contract No. MAT 93-793. We thank R. Sáez-Puche for the preparation of the samples used in this work. A.L. acknowledges the European Union under Contract No. ERBCHBICT941659. C.T. acknowledges discussions with B. Dareys and P. Thurian.

[1] A. Salinas-Sánchez, J. L. García-Muñoz, J. Rodríguez-Carvajal, R. Sáez-Puche, and J. L. Martínez, J. Solid State Chem. **100**, 201 (1992).

[2] A. Salinas-Sánchez and R. Sáez-Puche, Solid State Ion. **63-65**, 927 (1993); see also T. Mochiku *et al.*, J. Phys. Soc. Jpn. **60**, 1959 (1991).

[3] M. Taibi, J. Aride, J. Darriet, A. Moqine, and A. Boukhari, J. Solid State Chem. **86**, 233 (1990); H. K. Müller and S. Möhr, J. Less-Common Met. **170**, 127 (1991).

[4] A. de Andrés, S. Taboada, J. L. Martínez, A. Salinas, J. Hernández, and R. Sáez-Puche, Phys. Rev. B **47**, 14 898 (1993).

[5] M. V. Abrashev, G. A. Zlateva, M. N. Iliev, and M. Gyulmezov, Phys. Rev. B **49**, 11 783 (1994).

[6] S. Taboada, A. de Andrés, J. E. Muñoz Santiuste, C. Prieto, J. L. Martínez, and A. Criado, Phys. Rev. B **50**, 9157 (1994).

[7] E. T. Heyen, R. Wegerer, E. Schönherr, and M. Cardona, Phys. Rev. B **44**, 10 195 (1991).

[8] J. A. Sanjurjo, G. B. Martins, P. G. Pagliuso, E. Granado, Y. Torriani, C. Rettori, S. Oseroff, and Z. Fisk, Phys. Rev. B **51**, 1185 (1995).

[9] P. Dufour, S. Jandl, C. Thomsen, M. Cardona, B. M. Wanklyn, and C. Changkang, Phys. Rev. B **51**, 1053 (1995).

[10] M. Taibi, J. Aride, E. Antic-Fidancev, M. Lemaitre-Blaise, and P. Porcher, Phys. Status Solidi A **115**, 523 (1989).

[11] G. F. Koster, J. O. Dimmoch, R. G. Wheeler, and H. Statz. *Properties of the Thirty-two Point Groups* (MIT Press, Cambridge, 1965).

[12] G. Blasse, in *Solid State Luminescence, Theory, Materials and Devices*, edited by A. H. Kitai (Chapman & Hall, London, 1993).